



Artificial Muscles from Hybrid Carbon Nanotube-Polypyrrole-Coated Twisted and Coiled Yarns

Shazed Aziz, Jose G. Martinez, Javad Foroughi, Geoffrey M. Spinks, and Edwin W. H. Jager*

Electrochemically or electrothermally driven twisted/coiled carbon nanotube (CNT) yarn actuators are interesting artificial muscles for wearables as they can sustain high stress. However, due to high fabrication costs, these yarns have limited their application in smart textiles. An alternative approach is to use off-the-shelf yarns and coat them with conductive polymers that deliver high actuation properties. Here, novel hybrid textile yarns are demonstrated that combine CNT and an electroactive polypyrrole coating to provide both high strength and good actuation properties. CNT-coated polyester yarns are twisted and coiled and subjected to electrochemical coating of polypyrrole to obtain the hierarchical soft actuators. When twisted without coiling, the polypyrrole-coated yarns produce fully reversible 25° mm^{-1} rotation, $8.3\times$ higher than the non-reversible rotation from twisted CNT-coated yarns in a three-electrode electrochemical system operated between $+0.4$ and -1.0 V (vs Ag/AgCl). The coiled yarns generate fully reversible 10° mm^{-1} rotation and 0.22% contraction strain, $2.75\times$ higher than coiled CNT-coated yarns, when operated within the same potential window. The twisted and coiled yarns exhibit high tensile strength with excellent abrasion resistance in wet and dry shearing conditions that can match the requirements for using them as soft actuators in wearables and textile exoskeletons.

1. Introduction

The combination of technological advances in mechanical, mechatronic, and materials science and engineering has resulted

Dr. S. Aziz, Dr. J. G. Martinez, Dr. E. W. H. Jager
Division of Sensor and Actuator Systems, Department of Physics
Chemistry and Biology (IFM)
Linköping University
Linköping SE-581 83, Sweden
E-mail: edwin.jager@liu.se

Dr. J. Foroughi, Prof. G. M. Spinks, Dr. E. W. H. Jager
Australian Institute for Innovative Materials
University of Wollongong
Innovation Campus, Squires Way, North Wollongong, NSW 2522,
Australia

The ORCID identification number(s) for the author(s) of this article can be found under <https://doi.org/10.1002/mame.202000421>.

© 2020 The Authors. Published by Wiley-VCH GmbH. This is an open access article under the terms of the Creative Commons Attribution-NonCommercial License, which permits use, distribution and reproduction in any medium, provided the original work is properly cited and is not used for commercial purposes.

DOI: 10.1002/mame.202000421

in the significant progress in soft-robotics, flexible prosthetics, and exoskeletons that either boost human performance or assist disabled people in carrying out day-to-day tasks. One of the significant innovations is introducing soft and lightweight actuating materials (artificial muscles) that can mimic biological muscles and operate smoothly and silently.^[1] The current materials of interest for artificial muscles are carbon nanotubes (CNT),^[2] graphene,^[3] shape memory alloys (SMA),^[4] shape memory polymers (SMP),^[5] conductive polymers,^[6] and highly oriented polymer yarns^[7] that can be induced thermally, chemically, photonicallly, or electrochemically to obtain muscle-like actuation. Artificial muscles made from polymeric or nano-carbon-based yarns can find versatile applications ranging from assistive wearable artificial muscles for biomedical rehabilitation or assistance for daily activities, bioinspired and biomimetic systems, for handling delicate objects, and on-demand movement.^[8]

CNT yarn actuators are of great interest in the field of electrochemically or electrothermally induced wearable artificial muscle technologies.^[2a,9] These actuators exhibit excellent mechanical properties needed for wearable textile exoskeletons.^[2c,10] Recently, the feasibility of using multi-walled CNT forest drawn twisted or coiled yarns was demonstrated in terms of both tensile and rotational actuation. As high as 3% tensile actuation and $12.6^\circ \text{ mm}^{-1}$ rotational actuation was reported from an electrothermally activated twist-spun wax-filled CNT yarn when subjected to $25\text{--}210^\circ \text{C}$ temperature variations.^[9c] On the other hand, electrochemically induced twist-spun CNT yarns have shown a maximum of $180^\circ \text{ mm}^{-1}$ torsional rotation and 0.7% axial strain in an organic electrolyte (0.2 M tetrabutylammonium hexafluorophosphate (TBA.PF6) in acetonitrile) when pulsed from -2.0 to $+2.0$ V versus Ag/Ag⁺ reference.^[9b]

However, due to the reasonably high cost associated with their fabrication, these CNT yarn actuators have limited practicability in smart textiles where low cost is desirable. Therefore, the interest in using inexpensive textile yarns has grown. Several researchers have shown the feasibility of using such yarns to construct simple textile actuators actuated by thermal,^[7b] electrothermal,^[9a] electronic,^[11] electrochemical,^[9b,12] or electrical^[9c] energy inputs. Similar to CNT yarn muscles, twisted and coiled textile yarns

of nylon 6,6 have shown thermally or electrothermally operated reversible tensile and rotational actuation of 12.5% and 5° mm^{-1} , respectively, when the temperature was altered between 20 and 120°C .^[7b] Another promising strategy has been demonstrated that utilizes the coating of conductive polymers to deliver the electrochemically driven actuation of the textile yarns. It was shown that the multilayer chemical and electrochemical coating of poly(3,4-ethylenedioxythiophene) PEDOT-polypyrrole (PPy) on commercial cellulose based single yarn could produce 0.075% linear actuation when a square wave potential (+0.5 and -1.0 V) was applied. The strain was shown to be further increased to 3% by using a knitted fabric made of the same yarns, that is, a 53-fold amplification of the strain due to the textile architecture.^[12] Researchers have also utilized commercially available conductive yarns to electrochemically coat with PPy providing a reversible 0.05% linear actuation within the potential difference of 0.1 and -1.0 V (vs Ag/AgCl) in a 0.1 M aqueous NaDBS electrolyte media.^[13]

Electrochemically actuated CNT-coated yarns depend mainly on the volume expansion caused by double-layer charge injection where the extent of volume expansion can be increased by using a suitable conductive polymer coating. For example, PPy undergoes a volume change upon electrochemical oxidation or reduction by applying a low potential of 1–2 V. The reversible volume change is predominantly caused by the insertion or ejection of ions and solvent molecules into the polymer structure. This volume change is used to build actuators in different geometry and sizes.^[6b,14] While conductive polymer actuators display a large stress generation, ≈ 10 times higher than that of a mammalian muscle,^[15] strain is still limited. We here demonstrate novel hybrid textile yarns with hierarchical structures that merge both the excellent mechanical strength of CNT and high electroactivity of polypyrrole to provide both high strength and good actuation properties. The sustainability of electrical conductivity of these yarn actuators is also demonstrated in wet and dry shearing conditions. In order to focus on the electro-mechanical actuation properties of the CNT and PPy layers and simplify the system, the yarn actuators are operated in aqueous NaDBS electrolyte, which is commonly used in CP actuators and ensures cation-driven actuation only.^[14b,16] The aqueous electrolyte is chosen over their organic counterparts as

this exhibits negligible toxicity and flammability.^[17] However, the ultimate goal is to achieve operation in ambient air actuation by using ionogel-based electrolytes.^[18] It is anticipated that our future work will embed the yarn actuators in ionogels to achieve all-solid-state actuation. The aqueous electrolyte from current work will be used as the precursor material of ionogel solid electrolyte.

2. Results and Discussion

2.1. Electrochemical Characteristics

Commercially sourced polyethylene terephthalate (PET) textile yarn (0.2 mm diameter) was initially coated with CNT sheet that was obtained from a spinnable CNT forest. These CNT-PET yarns were mechanically twisted and coiled. Electrical characterizations of the twisted and coiled CNT-PET yarns showed that all the samples had a conductivity within the range of $150\text{--}1200 \text{ S m}^{-1}$. Considering the previously reported works,^[13] this conductivity range was found suitable for electrochemical deposition of PPy. The PPy coating was obtained in 0.1 M NaDBS and 0.1 M pyrrole aqueous solution by applying a constant current of $5 \mu\text{A}$ through the yarns of the different materials for 2 h. **Figure 1** shows the characteristic curves of electrochemical deposition of PPy(DBS) on CNT-PET yarns and the corresponding CV curves before and after the coating process. Figure 1A shows the development of the potential of the yarn during the electrochemical polymerization process. All potential transients exhibited an initial increment followed by a slight decrease of the potential, which should correspond with a standard electrochemical polymerization process starting with the nucleation of the PPy and the subsequent PPy growth.^[19] The successful deposition of highly conductive PPy(DBS) on the untwisted, twisted, and coiled CNT-PET yarns was confirmed from the CV tests where the flow of current was increased from $6 \mu\text{A}$ before to $70 \mu\text{A}$ after the coating process (Figure 1B). Redox peaks (or clear changes in the current/potential slope) could be observed in the CV curves pointing to the presence of a significant amount of electrochemically active polymer on the CNT-PET/PPy yarn surface.

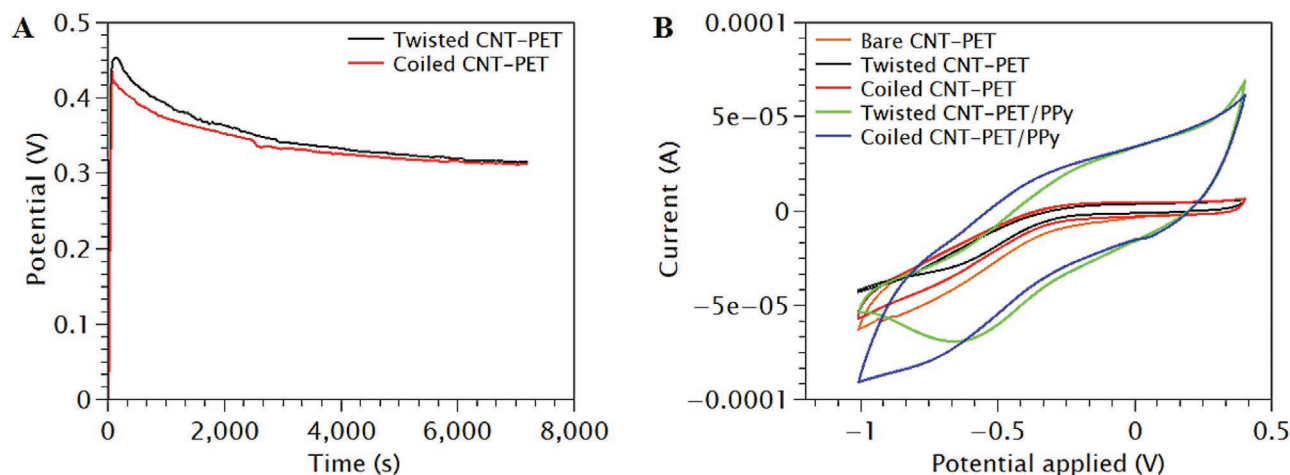


Figure 1. Electrochemical properties of yarn muscles: A) potential generated during electrochemical polymerization at $5 \mu\text{A}$ current and B) cyclic voltammetry of CNT-PET and CNT-PET/PPy yarns.

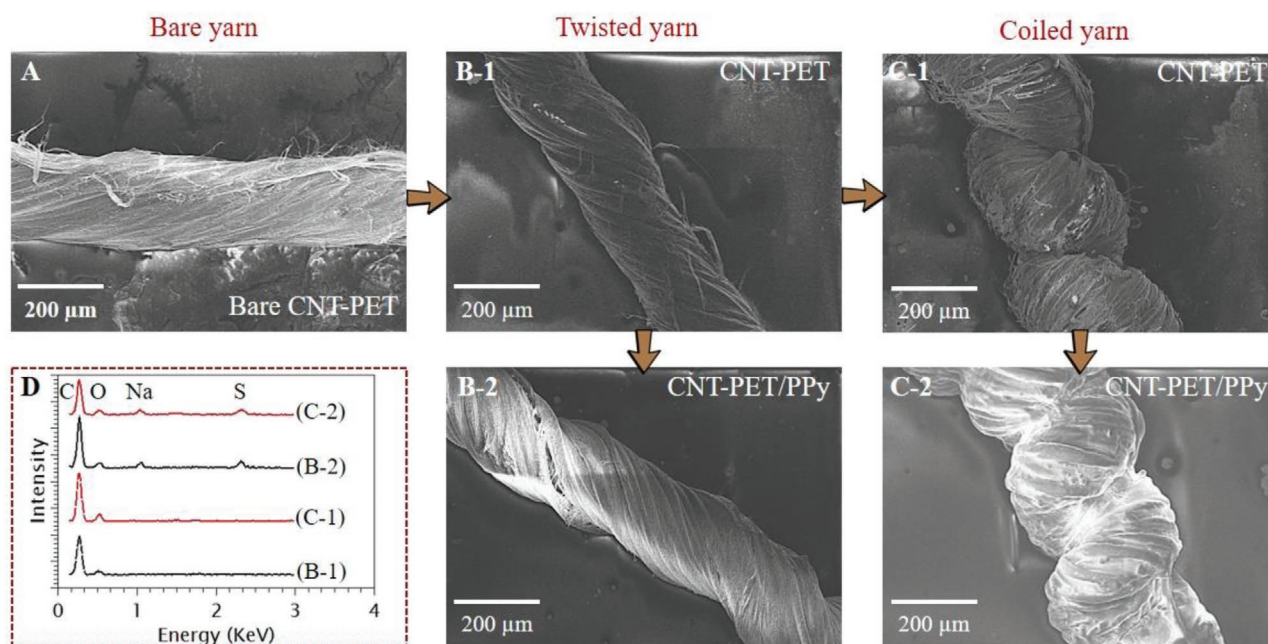


Figure 2. SEM images of yarn muscles: A) CNT-coated untwisted PET yarn, B-1,B-2) highly twisted CNT-PET yarn and CNT-PET/PPy yarn, C-1,C-2) twist-induced coiled CNT-PET yarn and CNT-PET/PPy yarn. Panel (D) shows the surface elemental composition of as-fabricated yarn muscles.

2.2. Surface Morphology and Mechanical Properties

Figure 2 shows the SEM images of differently structured CNT-PET yarns before and after the PPy(DBS) coating. The coating is visually noticeable by comparing the surface uniformity and yarn thicknesses. PPy(DBS) coating is highly uniform on the yarn surface and bonded to the CNT-PET filaments, similar to the CNT-coated carbon fiber reinforced composites.^[20] In this multi-scale reinforcement, CNT forest has also acted as the additional supporting reinforcement within the PPy matrix. Further validation of polymer coating was conducted by EDX analysis as shown in the inset of Figure 2. The significant rise of sodium and sulfur peaks points to the presence of NaDBS that corresponds with the dopants present in the PPy (DBS is trapped in PPy as the dopant and Na is the mobile counter ion exchanged to keep the electroneutrality). The N peak is usually much smaller and often hard to differentiate from C and O.^[21]

The mechanical properties of the yarn muscles were also evaluated in both dry and wet states within a specific stress–strain range that could affect the actuation properties (Figure S1, Supporting Information). The fundamental mechanical properties are listed in Table 1. For all types of yarns, Young's modulus, tensile stiffness, and extent of elastic recovery have decreased when tested in NaDBS wet media. The phenomenon agrees to

the conventional actuation principle of twisted/coiled artificial muscles where the stiffness is typically altered by the actuation stimulus, such as heat, light, electric field, or change in the chemical environment as well as a change in the PPy properties in solvents.^[22] Next, we investigated the yarn's actuation ability upon on electrochemical charge injection. In general, the stiffness (S) of helical coils is defined by the contributing yarn diameter (d), coil diameter (D), number of turns in the coil (N), and the material's shear modulus (G)^[23]

$$S = \frac{Gd^4}{8D^3N} \quad (1)$$

The change in stiffness of coiled muscles is usually determined by the competing effects of the decrease in elastic modulus and the increase in yarn diameter that co-occur during the electrochemical charging in an aqueous media.

2.3. Actuation Test Results

Several electrochemically induced actuation cycles were performed to evaluate the torsional actuation of the yarn muscles in 0.1 M NaDBS aqueous solution (Figure 3). Figure 3A shows

Table 1. Mechanical properties of yarn muscles (extracted from Figure S1, Supporting Information).

Yarn types →	Bare CNT-PET		Twisted CNT-PET		Coiled CNT-PET		Twisted CNT-PET/PPy		Coiled CNT-PET/PPy	
	Dry	Wet	Dry	Wet	Dry	Wet	Dry	Wet	Dry	Wet
Young's modulus [MPa]	466.3	408.3	719.6	631.4	14.6	11.6	570.8	375.9	12.5	8.2
Tensile stiffness [N m ⁻¹]	488.3	427.6	610.6	535.6	61.1	47.6	659.0	433.0	66.9	43.3
Elasticity in the strained zone [%]	88	100	88	100	88	100	97	87	97	87

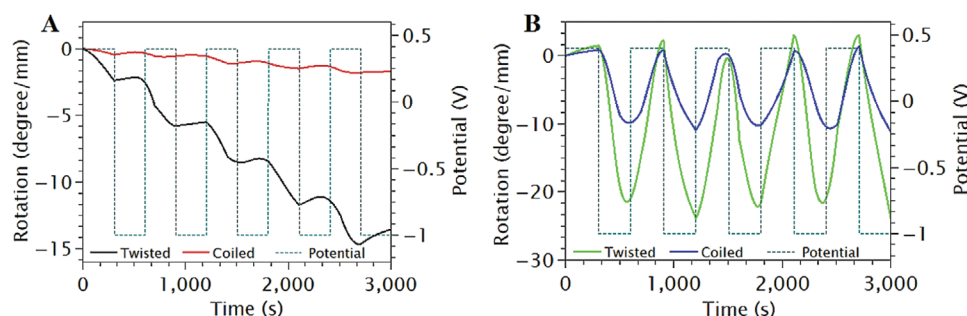


Figure 3. Electrochemically induced torsional actuation of yarn muscles: A) CNT-PET yarns and B) CNT-PET/PPy yarns.

the five consecutive cycles of torsional rotation obtained from twisted and coiled CNT-PET yarns. A non-reversible and small degree of reversible rotation was observed from coiled yarn whereas twisted yarn produced a higher rotation, again without full reversibility. The partial untwisting/retwisting of the CNT-PET yarn if due to the positive or negative electrochemical charge injection as described by Foroughi et al.^[9b] The application of a positive potential caused untwist in the CNT coated yarn with some recovered uptwist when the potential was negative. When positively charged, the CNT coating increased in volume and with good adhesion to the underlying yarn, this volume increase caused the entire CNT-PET structure to untwist. The non-reversible phenomenon was observed by previous researchers^[9b] when immersing a twisted multi-walled neat CNT yarn, and a counter electrode in an electrolyte and applying a voltage between these electrodes causes the yarn to untwist partially. The torque produced by the reduction in CNT coating volume with negative electrochemical charging was not enough to retwist the thermally annealed twisted or coiled CNT-PET yarn. However, as can be seen in Figure 3A, cycling between a smaller voltage window such as 0.4 and 0 V would have produced a more reversible torsional actuation, although of smaller magnitude. Less torsional rotation observed in the coiled structures is expected as the untwisting of the helical yarn converts to the linear actuation of the coiled yarn,^[7b] and the final rotation is contributed by the uncoiling phenomenon.^[24]

Significantly larger torsional rotation with full reversibility was obtained from twisted and coiled CNT-PET/PPy yarns in 0.1 M NaDBS aqueous solution providing 25° and 10° rotation per millimeter of sample lengths, respectively (Figure 3B). Unlike CNT-PET yarns, the untwisting happened in CNT-

PET/PPy yarns when a negative potential was applied. Here, the PPy(DBS) was being reduced in the negative potential and swelled due to the incorporation of Na⁺ ions. Again, the volume expansion of the coating encouraged untwisting of the yarn. The PPy(DBS) coating swelled to a greater extent than the CNT coating and the amount of swelling is proportional to the torsional stroke. Low stiffness of CNT-PET/PPy yarns also improved the torque balance during the retwisting process due to the negative charge injection that increased the reversibility of torsional rotation.

Smaller torsional rotation obtained from both the CNT-PET and CNT-PET/PPy coiled yarn compared to the twisted can be explained in terms of torque balance where electrochemical charging of the system had to withstand the torque associated with both twisted and coiled structures. Again, compared to CNT coating, the extent of swelling of PPy coating of the coiled is higher that primarily contributes to higher torsional stroke. One of the key features that both the twisted and coiled CNT-PET/PPy yarns exhibit is the complete torsional actuation reversibility starting from the first cycle that is rarely found in the electrochemical actuator systems.

Next, the ability of the coated yarns to electrochemically induce linear actuation was evaluated (Figure 4). Figure 4A shows ten consecutive cycles of actuation obtained from CNT-PET yarn muscles when a square potential wave of -1.0 to 0.4 V vs Ag/AgCl was applied. Twisted CNT-PET yarn showed a tiny but reversible 0.008% actuation whereas coiling the same length of yarn increased the actuation strain by a factor of 10 providing more than 0.08% lengthwise contraction/expansion. It was noted that the yarns underwent length contraction when the positive charge was applied, and vice versa. The insight of the length direction contraction/expansion is obtained by

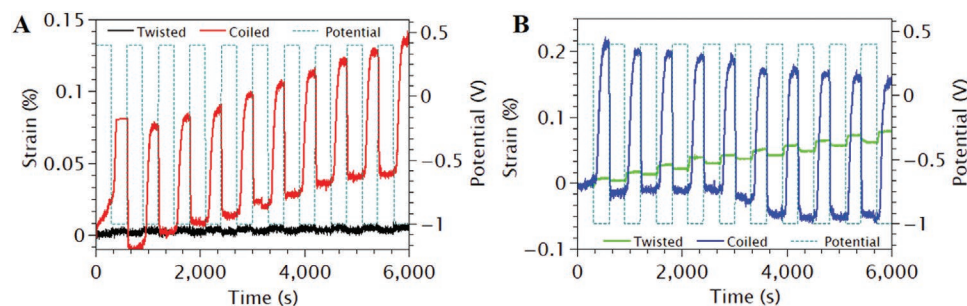


Figure 4. Electrochemically induced linear actuation of yarn muscles biased at 20 mN external force when square potential waves (-1.0, 0.4 V vs Ag/AgCl) were applied in 0.1 M NaDBS aqueous solution: A) CNT-PET yarns and B) CNT-PET/PPy yarns.

noting that large positive or negative electrochemical charge injection produces partial untwisting/retwisting of highly twisted multi-walled CNT yarn if that is free to rotate. However, the length-direction contraction was evidenced for a twisted CNT yarn tethered at both ends so that it cannot rotate.^[9b] In the context of this work, CNT yarn is helically wrapped around the non-electroactive PET yarn surface that exhibits comparatively smaller charge injection and results in negligible linear contraction. On the other hand, the electrochemically induced fiber untwist phenomenon drives the length change for coiled yarns by changing the bias angle described by the spring mechanics theories.^[9b] When coiled, the linear contraction of the straight twisted yarns happens through the coil helix direction due to some untwisting of the yarn.^[7b,9b,9c]

Figure 4B shows the actuation strain cycles of twisted and coiled CNT-PET/PPy yarns providing 0.02% and 0.22% reversible contraction/expansion, respectively. In the cases of twisted and coiled CNT-PET/PPy yarn actuation, the actuation behavior remains similar: length contraction when a positive potential is applied and expansion when a negative one. However, this behavior occurs in the opposite direction to that observed in the CNT-PET yarns when the coating volume is considered. Application of the negative potential in an aqueous NaDBS electrolyte media caused the polypyrrole to reduce resulting in a significant expansion, and vice versa in the positively charged oxidized state.^[25] Whereas, an increase in coating volume generally causes yarn untwist and a consequent length contraction in coiled yarns, the CNT-PET/PPy coiled yarns tended to increase in length as the coating volume increased. In coiled CNT-PET/PPy yarn, electropolymerized polypyrrole was in contact between coil turns so that the distance between coil turns increased as the PPy(DBS) coating swelled. The inter-coil polymer stretches coiled structure and restricted the untwisting/retwisting process that is key for the linear expansion/contraction. The contraction/expansion results solely from the Na⁺ cation-driven volume shrinkage/expansion of the inter-coil PPy(DBS) (DBS is trapped in PPy as the dopant).^[14b,16] Once oxidized, the shrinkage of PPy(DBS) allowed the coils to reform in their preliminary unstretched length. Reduction of the polymer caused volume expansion and brought the coiled muscle in stretched form. In this context, the extent of linear contraction depends only on the amount of inter-coil polymer. Since the ion-driven PPy(DBS) exhibits completely reversible volume alteration, the linear actuation of the coiled muscles has been found to be fully reversible. The actuation process for both CNT-PET and CNT-PET/PPy yarns was significantly fast allowing the yarns to contract/expand within a few seconds of charge injection (Figure S2, Supporting Information).

In this work, we measured the actuation performance for ten cycles without considering the frequency response. However, it has been demonstrated previously that these conductive polymer actuators can show improved actuation speed (i.e., high frequency operation)^[26] and long life time of tens of thousands cycles.^[27] Embedding the conductive polymer-coated yarns into a textile construction will also lead to a significant improvement of the cycle life time.^[12] Scalable and high-frequency response can be obtained by using thinner CP layers.^[26] However, as applicable to most linear artificial muscles, thinner active material will provide higher speeds, but the generated

stress will be consequently decreased as the exerted force depends on the cross-sectional area of the active (stress generating) material.^[23,28] A practical way of producing the actuators with high stress and high strain is by parallel assembling of many yarns or fibers using advanced textile processing, such as knitting and weaving of yarn actuators.^[12]

2.4. Abrasion Test Results

Wet and dry state abrasion tests were performed to investigate the sustainability of the CNT and conductive PPy(DBS) coating on PET yarn surface. This test is not only crucial for liquid electrolyte based operations, it also offers essential insights for solid electrolyte based operations, i.e., when embedded in an ionogel for in-air operation. When, e.g., used in wearable devices, the yarn actuators will be subjected to external tensile or torsional loading. This external load can transmit to the yarn/gel interface and eventually lead to a delamination of the conductive polymer layer also when embedded in an ionogel. The ionogel coating on PPy layer may also be delaminated induced by temperature changes or substrate bending. A covalent chemical bonding between the layers could be introduced to achieve permanent layer-layer attachment.^[18a,29] Different strategies on how the counterelectrode will be implemented in the in-air configuration are currently being studied. Figure 6 shows the abrasion resistance test subjected to the yarn muscles and the corresponding electrical properties before and after abrasion. **Figure 5A** demonstrates the test method conducted for an example yarn (CNT-PET/PPy yarn) among all the five different muscle categories. The tests include multiple steps where each yarn was first stirred in distilled water at 120 rpm for 30 min, then dried for 60 min and finally, placed in between two plies of sticky tape where the plies were peeled separated to abrade the yarn. The yarns sustained after wet and dry abrasion showing no evidence of delaminated polypyrrole both in the water bath and sticky tape. **Figure 5B** shows the electrical properties of non-abraded and abraded yarns as calculated from the following equation

$$\sigma = \frac{l}{\rho} = \frac{l}{RA} \quad (2)$$

here, ρ is the resistivity, R is the electrical resistance, l is the yarn length, A is the yarn cross-sectional area (measured at the same yarn area before and after abrasion), and σ is the conductivity of the yarn. The small or no change of electrical conductivity measured before and after abrasion tests suggests that the multi-scale reinforcement has provided high interfacial shear strength in between the core PET yarn, CNT wrapping, and PPy coating interfaces.

Visual inspection of the abraded samples did not show significant changes in coating thickness and uniformity. The conductivity values also remained almost unchanged before and after abrasion. The phenomenon can be explained as a result of the branched CNT forest that acts as the bridge in between the core PET yarn and bulk PPy coating, creating a high surface area of the PPy to grow on/in, similar to the rough electroplated Au surfaces.^[30] The shear strength of the yarn-conductive polymer

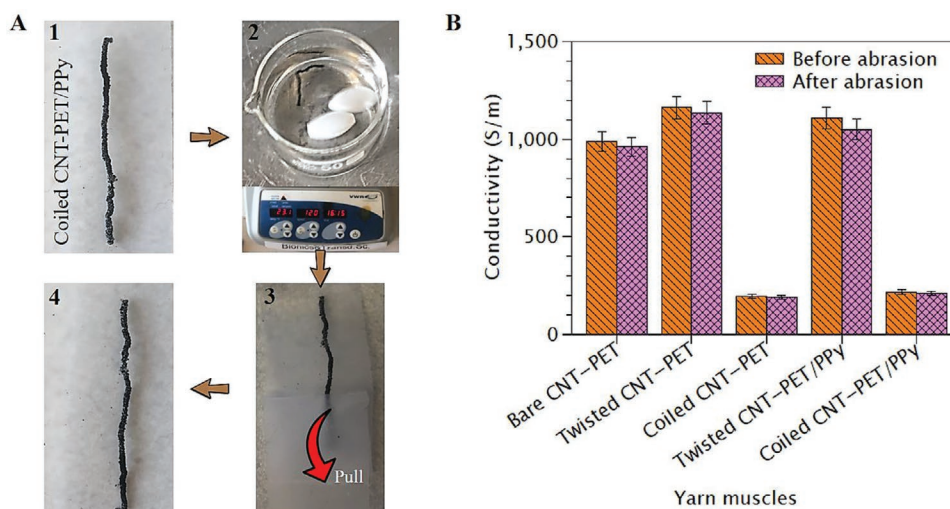


Figure 5. Electrical property of yarn muscles subjected to mechanical impacts: A) 1—an example dry CNT-PET/PPy yarn, 2—steered in water at 120 rpm for 30 min, 3—surface abrasion to dried yarn provided by highly sticky tape, 4—water-steered and abraded yarn sample. B) Electrical conductivity before and after abrasion.

interface was hence increased that prevented the delamination of polymer from the yarn surface.

3. Conclusion

Here, we present new yarn-based artificial muscles prepared from hybrid CNT-coated PET yarns that are electrochemically operated to provide a great combination of strength/actuation properties. CNT-coated PET textile yarns were mechanically twisted and coiled and subjected to the electrochemical coating of polypyrrole to obtain the hierarchical muscle structures. In the context of this work, multi-scale reinforcement of CNT and core textile yarn within the conductive polymer layer provided the overall actuation by utilizing a combination of the electrochemically activated double layer charge injection and volumetric expansion/contraction mechanism. Once twisted, the polypyrrole coated yarns produce fully reversible 25° mm^{-1} rotation, which is $8.3\times$ higher than the non-reversible 3° mm^{-1} rotation from twisted CNT-coated yarns. More significantly, the polypyrrole coated coiled yarn generated fully reversible 0.22% contraction, which is $2.75\times$ higher compared to 0.08% contraction of coiled CNT-coated yarn. Excellent abrasion resistance of the hybrid yarns under the wet and dry shearing conditions could make them useful as the functional components of reusable textiles. The actuation results of current work use an aqueous electrolyte to operate in. In future work, we will embed them in ionogels to achieve operation in ambient air actuation.^[18] The developed CNT-coated hybrid yarn actuators exhibit high mechanical properties that are of great interest for using them as soft actuators, or artificial muscles, in wearables and textile exoskeletons.

4. Experimental Section

Materials: Sodium dodecylbenzenesulfonate (NaDBS) from TCI Europe was used as received. Pyrrole (from SAFC, acquired through

Sigma-Aldrich) was distilled under vacuum before use and stored at -20°C . Ultrapure water was obtained from Milli-Q Plus water equipment and used for the experiments. PET yarn (100/34 D polyester yarn) was obtained from Shijiazhuang Yunchong Trading Co., Ltd., China. Spinnable multi-walled CNT forest was prepared as previously reported.^[9b] All the polymerization processes, electrochemical characterizations, and electrochemical actuation tests were performed in a single-compartment three-electrode electrochemical cell, connected to a potentiostat-galvanostat (Autolab PGSTAT101) from Metrohm AG, Switzerland. The input/output parameters were controlled by an electrochemistry software named NOVA 2.1.1. The reference electrode was a BASi MF-2052 Ag/AgCl (3 M NaCl) electrode. All potential values from electrochemical experiments in this work are referred to this electrode. A stainless-steel mesh having 6 cm^2 of surface area was used as the counter electrode. A force-displacement lever arm transducer (Aurora Scientific model 300B, Canada) was used to measure the real-time actuation responses both in isometric and isotonic modes. All the experiments were performed at room temperature (22°C).

Fabrication Method and Electrochemical Characterizations: A complete schematic procedure of the fabrication method of twisted/coiled CNT-PET and CNT-PET/PPy yarns is illustrated in Figure 6. Commercially sourced PET textile yarn (0.2 mm diameter) was initially coated with CNT sheet that was obtained from a spinnable CNT forest. A movable platform was used to cover the yarn surface with CNT while simultaneous low-extent fiber twisting was conducted to ensure enough interfacial strength (Figure 6A). The highly twisted structures were obtained by further twisting the CNT-PET yarns under 10 MPa stress until the offset of coiling, followed by the heat-setting of the yarn at 100°C for 60 min (Figure 6B-1). After cooling, the twisted structures sustained as a result of the newly formed helical crystal structures within the PET yarn. A few samples were further chosen to insert extreme twists that resulted in the formation of coils. The coiled yarns were further subjected to heat setting to ensure structural stability and robustness (Figure 6B-2). The two-step heating process provides the geometrical uniformity of the twisted structures within the over-twisted coils. Figure 6B-3 shows that the amount of contraction strain was more than 70% during the overall process of fabricating fully coiled yarns. Cyclic voltammetry (CV) tests were performed by alternatively applying 0.4 and -1 V potential for both twisted and coiled CNT-PET yarns to study qualitative information about electrochemical processes.

Thereafter, twisted and coiled yarn samples were subjected to constant current to perform the electrochemical polymerization process upon selecting the applied current from the CV curves of twisted/coiled

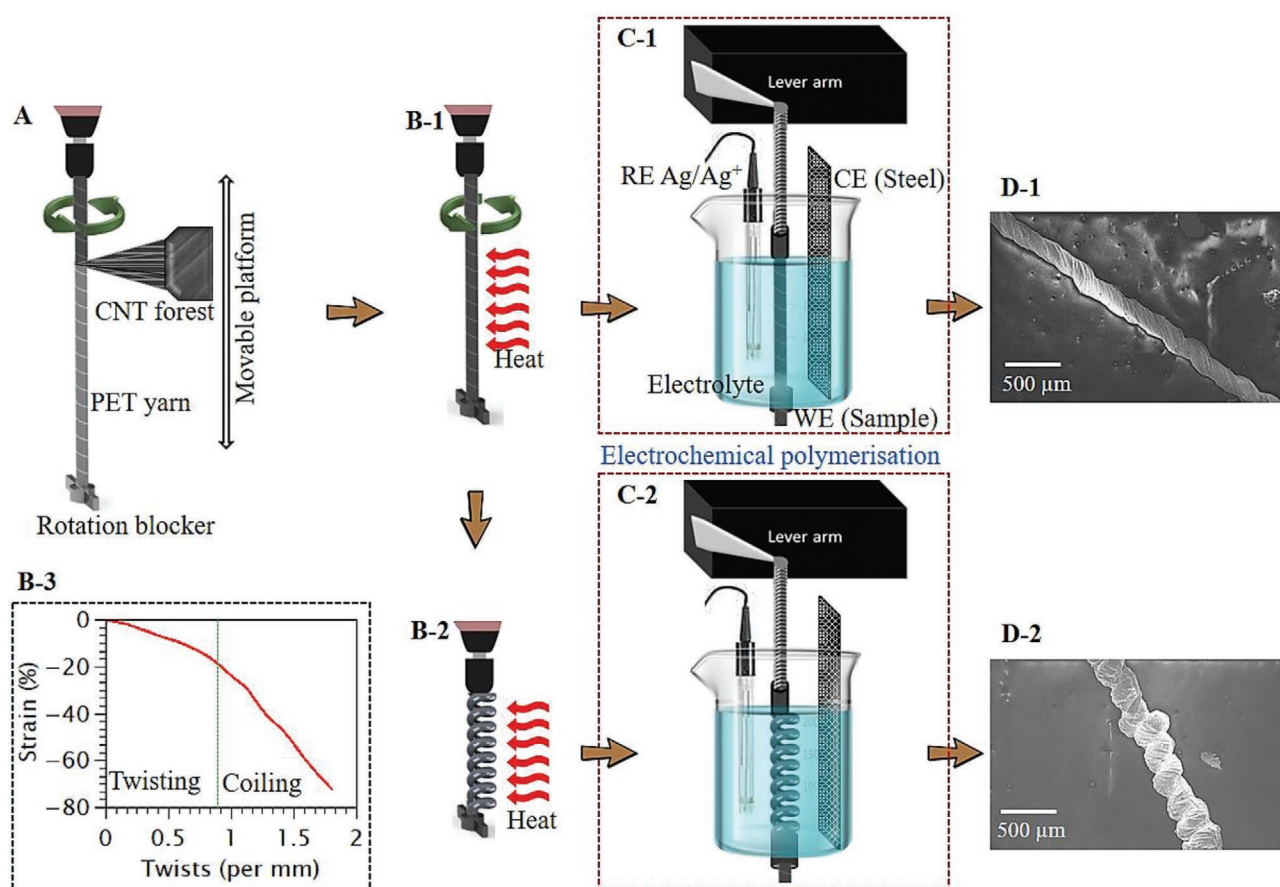


Figure 6. Schematic illustration of the fabrication steps of the hierarchical CNT-PET/PPy artificial muscles: A) coating of CNT forest onto the surface of PET yarn, B-1,B-2) fabrication of twisted and coiled CNT-PET structures, B-3) quantification of intrinsic length change during the twist-coil process, C-1,C-2) electrochemical polymerization of pyrrole on twisted and coiled CNT-PET samples, D-1,D-2) SEM micrographs of twisted and coiled CNT-PET/PPy samples.

CNT-PET yarns.^[31] The process was held in a plastic beaker where the bottom ends of the yarns that acted as working electrodes (WE) were kept fixed leaving a suspended section outside the cell through a closed epoxy-glued hole (Figure 6C-1,C-2). The PPy coating was obtained in 0.1 M NaDBS and 0.1 M pyrrole aqueous solution by applying a constant current of 5 μ A through the yarns of the different materials for 2 h. Length of the yarns was kept consistent by connecting them with an isometrically operated lever arm. In isometric mode, the lever arm force was initially set high enough to keep the actuator at a constant length. Once the process is completed, the PPy-coated yarns were microscopically characterized (Figure 6D-1,D-2). CV tests were also performed by alternatively applying 0.4 and -1 V potential, which is the typical potential window used for electrochemical characterization of PPy. The potential window depends on the material, electrolyte used (e.g., solvent, pH, concentration), and setup (e.g., counter electrode). For instance, at potentials lower than ≈ -1 V, H_2O is reduced and H_2 (g) bubbles are generated and at potentials higher than ≈ 0.5 V PPy is over oxidized and starts to degenerate and loses its conductivity.^[32]

Evaluation of Morphological, Elemental, and Mechanical Properties: Morphological characterization of the yarn muscles was conducted by using a scanning electron microscopy (SEM) (Leo 1550 Gemini) operating at 4.00 keV. Additionally, energy-dispersive X-ray (EDX) spectroscopy was used to evaluate the elements present on both CNT-PET and CNT-PET/PPy yarns. Mechanical properties of the yarn muscles were characterized by using the lever arm where force was applied/released to stretch/relax the connected yarns and the resultant stress-strain curves were used to evaluate Young's modulus and tensile stiffness.

Actuation Tests Procedure: Actuation strains of the yarn muscles were evaluated by using the similar test methods demonstrated in Figure 6C-1,C-2. Initially, each type of yarns was connected to the lever arm under a constant force (isotonic mode) of 20 mN to ensure the samples were held straight. In isotonic mode, the elongation of yarn actuators (ΔL) was measured using the lever arm transducer (Aurora Scientific model 300B, Canada) and the actuation strain was calculated thereafter ($\epsilon = \Delta L/L_0$). Step potentials (0.4 and -1 V) were applied to the electrochemical cell while the lever arm was measuring the real-time contraction/expansion strains.

Electrochemically induced torsional actuation of the yarn muscles was evaluated by vertically suspending them with a constant weight that applied 10 mN equivalent force in air. The video of the torsional rotation was recorded using a Dino-Lite Edge digital microscope controlled by DinoCapture 2.0 software (version 1.5.14.G). The lengths of the twisted and coiled samples were 50 and 20 mm, respectively, to ensure the consistent yarn length before and after coiling. The time for each contraction/expansion cycle was set for 10 min for all the test samples.

Evaluation of the Abrasion Resistance of CNT-PET and CNT-PET/PPy Yarns: Validation of uniform and durable conductive coating was checked by subjecting the yarn muscles to mechanical abrasion in the dry and wet state. The yarns were first abraded in a water bath together with constant steering of a stir bar (120 rpm). Following the wet-state abrasion, dried yarns were placed in between two plies of highly sticky Teflon tapes and abraded by separating the tapes. Electrical conductivities of the yarns were measured in both non-abraded and abraded samples to check their feasibility in harsh mechanical environments. These tests also provided some insights into the high interfacial shear strength in between the core yarn and the hybrid CNT-PPy coating.

Supporting Information

Supporting Information is available from the Wiley Online Library or from the author.

Acknowledgements

J.G.M. acknowledges Promobilia Foundation (F17603) for their financial support. J.G.M. and E.W.H.J. acknowledge financial support from the Swedish Government Strategic Research Area in Materials Science on Functional Materials at Linköping University (faculty grant SFO Mat LiU no. 2009-00971), the Swedish Research Council (2014-3079), Carl Trygger Foundation (CTS:17-215), and European Union's Horizon 2020 research and innovation program under grant agreement no. 825232 "WEAFING." E.W.H.J. wishes to thank the University of Wollongong's Visiting International Scholar Award.

Conflict of Interest

The authors declare no conflict of interest.

Keywords

artificial muscles, carbon nanotubes, conductive polymers, polymeric actuators, smart textiles

Received: July 8, 2020
Revised: August 10, 2020
Published online:

- [1] a) Y. Bar-Cohen, *Electroactive Polymer (EAP) Actuators as Artificial Muscles: Reality, Potential, and Challenges*, SPIE, Bellingham, WA **2001**; b) Q. Zhao, Y. Wang, H. Cui, X. Du, *J. Mater. Chem. C* **2019**, 7, 6493.
- [2] a) R. H. Baughman, C. Cui, A. A. Zakhidov, Z. Iqbal, J. N. Barisci, G. M. Spinks, G. G. Wallace, A. Mazzoldi, D. De Rossi, A. G. Rinzler, O. Jaschinski, S. Roth, M. Kertesz, *Science* **1999**, 284, 1340; b) M. Hughes, G. M. Spinks, *Adv. Mater.* **2005**, 17, 443; c) S. Shahidi, B. Moazzzenchi, *J. Text. Inst.* **2018**, 109, 1653.
- [3] a) H. Cheng, Y. Hu, F. Zhao, Z. Dong, Y. Wang, N. Chen, Z. Zhang, L. Qu, *Adv. Mater.* **2014**, 26, 2909; b) J.-H. Jung, J.-H. Jeon, V. Sridhar, I.-K. Oh, *Carbon* **2011**, 49, 1279; c) M. Kotal, J. Kim, K. J. Kim, I.-K. Oh, *Adv. Mater.* **2016**, 28, 1610.
- [4] a) W. Huang, *Mater. Des.* **2002**, 23, 11; b) A. M. E. Kady, A. E. Mahfouz, M. F. Taher, presented at 2010 5th Cairo Int. Biomedical Engineering Conf., Cairo, Egypt, December 2010; c) S. Kim, E. Hawkes, K. Choy, M. Joldaz, J. Foley, R. Wood, presented at 2009 IEEE/RSJ Int. Conf. on Intelligent Robots and Systems, St. Louis, MO, October 2009.
- [5] a) K. Takashima, J. Rossiter, T. Mukai, *Sens. Actuators, A* **2010**, 164, 116; b) K. Takashima, K. Sugitani, N. Morimoto, S. Sakaguchi, T. Noritsugu, T. Mukai, *Smart Mater. Struct.* **2014**, 23, 125005.
- [6] a) A. Fannir, R. Temmer, G. T. M. Nguyen, L. Cadiergues, E. Laurent, J. D. W. Madden, F. Vidal, C. Plesse, *Adv. Mater. Technol.* **2019**, 4, 1800519; b) D. Melling, J. G. Martinez, E. W. H. Jager, *Adv. Mater.* **2019**, 31, 1808210; c) E. Smela, *Adv. Mater.* **2003**, 15, 481.
- [7] a) S. Aziz, S. Naficy, J. Foroughi, H. R. Brown, G. M. Spinks, *Sens. Actuators, A* **2018**, 283, 98; b) C. S. Haines, M. D. Lima, N. Li, G. M. Spinks, J. Foroughi, J. D. W. Madden, S. H. Kim, S. Fang, M. Jung de Andrade, F. Göktepe, O. Göktepe, S. M. Mirvakili, S. Naficy, X. Lepró, J. Oh, M. E. Kozlov, S. J. Kim, X. Xu, B. J. Swedlove, G. G. Wallace, R. H. Baughman, *Science* **2014**, 343, 868.
- [8] N.-K. Persson, J. G. Martinez, Y. Zhong, A. Maziz, E. W. H. Jager, *Adv. Mater. Technol.* **2018**, 3, 1700397.
- [9] a) J. Foroughi, G. M. Spinks, S. Aziz, A. Mirabedini, A. Jeiranikhameneh, G. G. Wallace, M. E. Kozlov, R. H. Baughman, *ACS Nano* **2016**, 10, 9129; b) J. Foroughi, G. M. Spinks, G. G. Wallace, J. Oh, M. E. Kozlov, S. Fang, T. Mirfakhrai, J. D. W. Madden, M. K. Shin, S. J. Kim, R. H. Baughman, *Science* **2011**, 334, 494; c) M. D. Lima, N. Li, M. Jung de Andrade, S. Fang, J. Oh, G. M. Spinks, M. E. Kozlov, C. S. Haines, D. Suh, J. Foroughi, S. J. Kim, Y. Chen, T. Ware, M. K. Shin, L. D. Machado, A. F. Fonseca, J. D. W. Madden, W. E. Voit, D. S. Galvão, R. H. Baughman, *Science* **2012**, 338, 928.
- [10] M. Miao, *Carbon Nanotube Fibres and Yarns for Smart Textiles: Production, Properties and Applications in Smart Textiles*, Woodhead Publishing, Oxford **2019**.
- [11] J. Guo, C. Xiang, T. Helps, M. Taghavi, J. Rossiter, presented at 2018 IEEE Int. Conf. on Soft Robotics (RoboSoft), Livorno, Italy, April 2018.
- [12] A. Maziz, A. Concas, A. Khaldi, J. Stålhand, N.-K. Persson, E. W. H. Jager, *Sci. Adv.* **2017**, 3, e1600327.
- [13] J. G. Martinez, K. Richter, N.-K. Persson, E. W. H. Jager, *Smart Mater. Struct.* **2018**, 27, 074004.
- [14] a) E. W. H. Jager, O. Inganäs, I. Lundström, *Science* **2000**, 288, 2335; b) E. Smela, *J. Micromech. Microeng.* **1999**, 9, 1.
- [15] K. J. Kim, S. Tadokoro, in *Electroactive Polymers for Robotic Applications*, Springer, London **2007**, p. 121.
- [16] a) Q. Pei, O. Inganaes, *J. Phys. Chem.* **1992**, 96, 10507; b) L. Bay, N. Mogensen, S. Skaarup, P. Sommer-Larsen, M. Jørgensen, K. West, *Macromolecules* **2002**, 35, 9345.
- [17] L. Xia, L. Yu, D. Hu, G. Z. Chen, *Mater. Chem. Front.* **2017**, 1, 584.
- [18] a) Y. Zhong, G. T. M. Nguyen, C. Plesse, F. Vidal, E. W. H. Jager, *ACS Appl. Mater. Interfaces* **2018**, 10, 21601; b) Y. Zhong, G. T. M. Nguyen, C. Plesse, F. Vidal, E. W. H. Jager, *J. Mater. Chem. C* **2019**, 7, 256.
- [19] J. G. Martinez, M. Ayán-Varela, J. I. Paredes, S. Villar-Rodil, S. D. Aznar-Cervantes, T. F. Otero, *ChemElectroChem* **2017**, 4, 1487.
- [20] S. Aziz, S. A. Rashid, S. Rahmanian, M. A. Salleh, *Polym. Compos.* **2015**, 36, 1941.
- [21] T. F. Otero, J. G. Martinez, *Adv. Funct. Mater.* **2014**, 24, 1259.
- [22] S. Skaarup, L. Bay, K. West, *Synth. Met.* **2007**, 157, 323.
- [23] G. M. Spinks, *J. Mater. Res.* **2016**, 31, 2917.
- [24] A. Mirabedini, S. Aziz, G. M. Spinks, J. Foroughi, *Soft Rob.* **2017**, 4, 421.
- [25] Q. Pei, O. Inganäs, *Synth. Met.* **1993**, 57, 3718.
- [26] A. Maziz, C. Plesse, C. Soyer, C. Chevrot, D. Teyssié, E. Cattani, F. Vidal, *Adv. Funct. Mater.* **2014**, 24, 4851.
- [27] J. D. Madden, D. Rinderknecht, P. A. Anquetil, I. W. Hunter, *Sens. Actuators, A* **2007**, 133, 210.
- [28] G. M. Spinks, S. E. Bakarich, S. Aziz, B. Salahuddin, H. Xin, *Sens. Actuators, A* **2019**, 290, 90.
- [29] S. W. Lee, H. J. Lee, J. H. Choi, W. G. Koh, J. M. Myoung, J. H. Hur, J. J. Park, J. H. Cho, U. Jeong, *Nano Lett.* **2010**, 10, 347.
- [30] a) C. C. Bohn, M. Pyo, S. Sadki, E. Smela, J. R. Reynolds, A. B. Brennan, presented at SPIE's 9th Annual Int. Symp. on Smart Structures and Materials, San Diego, CA, July 2002; b) M. Pyo, C. C. Bohn, E. Smela, J. R. Reynolds, A. B. Brennan, *Chem. Mater.* **2003**, 15, 916.
- [31] S. Cosnier, A. Karyakin, *Electropolymerization: Concepts, Materials and Applications*, Wiley, Weinheim, Germany **2011**.
- [32] a) B. Krichke, M. Zagorska, *Synth. Met.* **1989**, 28, 257; b) T. F. Otero, M. Alfaro, V. Martinez, M. A. Perez, J. G. Martinez, *Adv. Funct. Mater.* **2013**, 23, 3929; c) I. Rodríguez, B. R. Scharifker, J. Mostany, *J. Electroanal. Chem.* **2000**, 491, 117.